Perspective on Distributed Acoustic Sensing for Seismic Activity Monitoring

María. R. Fernández-Ruiz[1], Marcelo A. Soto[2], Ethan F. Williams[3], Sonia Martin-Lopez[1], Zhongwen Zhan[3], Miguel Gonzalez-Herraez[1], and Hugo F. Martins[4]

[1]Department of Electronics, University of Alcalá, Alcalá de Henares, 28805, Spain;
[2]Department of Electronic Engineering, Universidad Técnica Federico Santa María, Valparaíso, 2390123, Chile
[3]Seismological Laboratory, California Institute of Technology, Pasadena, CA 91125-2100, USA;
[4]Instituto de Óptica, CSIC, 28006 Madrid, Spain

ABSTRACT

Continuous, real-time monitoring of surface seismic activity around the globe is of great interest for acquiring new insight in global tomography analyses and for recognition of seismic patterns leading to potentially hazardous situations. The already-existing telecommunication fiber optic network arises as an ideal solution for this application, owing to its ubiquity and the capacity of optical fibers to perform distributed, highly sensitive monitoring of vibrations at relatively low cost (ultra-high density of point sensors available with minimal deployment of new equipment). This perspective article discusses early approaches on the application of fiber-optic distributed acoustic sensors (DAS) for seismic activity monitoring. The benefits and potential impact of DAS technology in this kind of applications are here illustrated with new experimental results on teleseism monitoring based on a specific approach: the so-called chirped-pulse DAS. This technology offers promising prospects for the field of seismic tomography due to its appealing properties in terms of simplicity, consistent sensitivity across sensing channels and robustness. Furthermore, we also report on several signal processing techniques readily applicable to chirped-pulse DAS recordings for extracting relevant seismic information from ambient acoustic noise. The outcome presented here may serve as foundation for a novel conception for ubiquitous seismic monitoring with minimal investment.

1 INTRODUCTION

Optical fibers have been traditionally designed to propagate confined light over several tens of kilometers with minimum attenuation and distortion. The excellent features of optical fibers as a light propagation medium have allowed the development of long-haul broadband optical transmission systems around the globe. Nevertheless, their high light confinement and low power losses have made optical fibers also attractive for other specific applications, such as optical sensing. In many cases, *optical fiber sensors* [1] have shown comparative advantages with respect to traditional electronic sensors, providing unmatched performance in many critical applications. Furthermore, optical fibers offer the possibility of measuring an environmental variable at each location along its length with a given sharp spatial resolution. This is a unique

1

feature of the so-called *distributed optical fiber sensors* [2,3] which can provide the simultaneous monitoring of up to several hundred thousand independent sensing points over a single optical fiber. Since no other technology can allow similar features, distributed fiber sensors have found a wide range of potential applications, including structural health monitoring, gas and/or liquid leak detection along pipelines, chemical sensing, and many others.

Distributed optical fiber sensors are based on the natural scattering processes arising in optical fibers, including Brillouin, Raman or Rayleigh scattering [4,5]. Each of these scattering processes can give rise to distributed sensors with very specific features [3,6–13]. Whereas distributed fiber sensors have been traditionally developed for monitoring quasi-static (i.e. slow-varying) variables, several approaches have been developed in the last decade to monitor dynamic strain variations and vibrations using optical fibers. Among the different existing technologies, Rayleigh scattering combined with optical time-domain reflectometry (OTDR) [14] or optical frequency-domain reflectometry (OFDR) [15] has allowed the development of *distributed acoustic sensors* (DAS), offering the possibility to monitor vibrations along an optical fiber at readout frequencies in the kHz-range [3]. This unique feature of DAS systems has permitted a significant expansion of the range of potential applications of distributed fiber sensors. For instance, some proof-of-concept experiments and preliminary results reported in the literature have demonstrated the significant benefits that DAS technology can bring to the highly demanding field of seismology [16–22]. Indeed, the use of DAS interrogation systems and long sensing optical fibers can offer a unique and unmatched monitoring platform for seismology laboratories worldwide Note that DAS systems based on OFDR are more appropriate for sensing over relatively short sensing ranges (up to hundreds of meters) with high spatial resolutions. Although a few notable exceptions can be found [23,24], OFDR is therefore typically not best-suited for the application of interest in this manuscript; for this reason hereafter we only focus on OTDR-based DAS systems.

In this manuscript, we first review the application of DAS in seismology (Section 2). The properties and advantages that distributed acoustic sensing can bring to seismic activity monitoring are described in Section 2.1. An overview of the state of the art of DAS systems is presented in Section 2.2, providing a comparison of the offered performance of existing alternatives. The applications of DAS on seismological research carried out to date are also briefly summarized in Section 2.3. Then, in Section 3, we focus on the application of a novel DAS technology, namely chirped-pulse DAS, for seismic activity monitoring in particularly noisy environments, highlighting its advantages with respect to traditional techniques. In Section 3.1, we present experimental recordings of an earthquake occurred in Fiji Islands using an optical fiber network located in a densely populated city, namely in Pasadena (CA, USA), i.e., at > 9000 km from the earthquake epicenter. To the best of our knowledge, this is the first time seismic activity is recorded from an already-installed fiber in a metropolitan area. Results demonstrate that a DAS interrogation system based on linearly chirped probe pulses can provide reliable teleseismic detection under a realistic, highly noisy environment, even at a huge distance away from the earthquake epicenter. Additionally, here we also describe different multi-dimensional signal processing techniques suitable for opto-electronic noise reduction as well as for extracting the relevant ground-motion information and discriminate it from ambient noise. Results verify a fairly good matching of detected waveforms with those measured by a nearby seismometer, but with the advantage of providing spatial information. In Section 3.2, we review additional results of the use of chirped pulse DAS for seismicity; in this case from an ocean-bottom DAS. Finally, in Section 4, we comment on the futures challenges that DAS technology has to face for the practical re-purpose of the telecommunication fiber network into a distributed seismograph

network, as well as a perspective analysis of the future steps of DAS into the broad field of seismology.

2 DISTRIBUTED ACOUSTIC SENSING IN SEISMOLOGY APPLICATIONS

The field of distributed acoustic sensing is gaining increasing interest worldwide due to the rising demands of distributed strain measurements in areas such as oil and gas industry, aeronautics, civil engineering, and more. This growing attention has encouraged research towards a more robust, precise and competitive sensing technology, producing a significant development in the last few years. The improved performance of DAS has unveiled their strong potential to become a routine instrument in geophysics studies, providing an excellent platform for data acquisition in terms of waveform fidelity, bandwidth, simplicity and cost-effectiveness. Although still incipient, the use of DAS for seismic monitoring is growing rapidly, with very optimistic projections to play a fundamental role in the next generation seismic networks.

2.1 BENEFITS OF DAS OVER TRADITIONAL SEISMOGRAPH POINT SENSORS

Conventional sensors in seismology are punctual seismographs. A seismograph is an instrument that detects and records ground motion along the three spatial dimensions. A single seismograph is enough to determine the presence of an earthquake through detection of different seismic waves (e.g., body or surface waves). For several decades, seismic tomography has relied on array configurations of synchronized seismic stations (i.e., seismographs) for extracting information aimed at the understanding of the Earth's structure and the processes that give rise to earthquakes [25]. A vast number of array seismograph configurations are currently spread around the globe, either at certain locations of interests [26,27] or locally deployed for temporary campaigns [28] (Fig. *1*). Seismic arrays provide information susceptible to be analyzed using special digital signal processing techniques, such as beamforming, to reveal information beyond earthquake monitoring, including quantification of active wave sources, determination of structures and processes occurring in the deep Earth, earthquake/tsunami early warning, tracking of wave field properties in volcanic areas, etc.
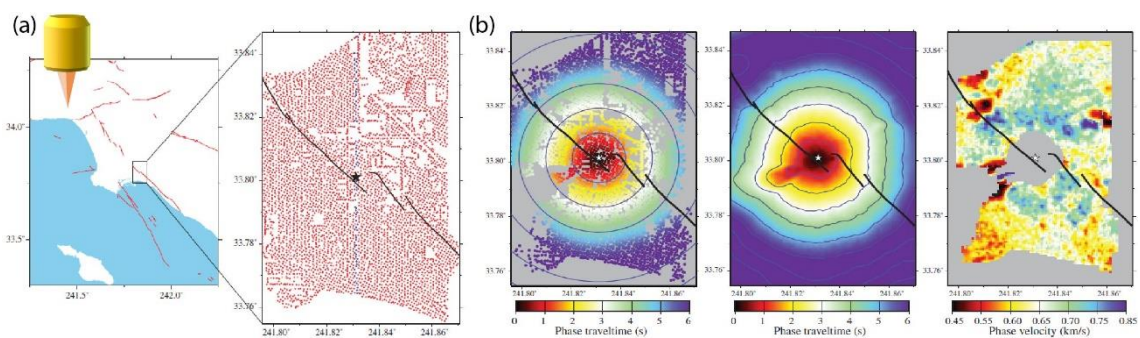

Fig. 1. (Extracted from Ref. [28]). (a) Array configuration of temporary seismic stations in Southern California. The array has >5000 sensors within a 5 km x 10 km area. Each red dot in the figure at the right shows a single seismograph. An example of a single seismograph is depicted in the upper left corner. (b) A demonstration of eikonal tomography, showing 1 Hz Rayleigh waves phase traveltime observed across the array in points with sufficiently high SNR (left figure) and interpolation of those results (middle figure) and phase velocity map based on the eikonal equation (right).

The permanent seismic arrays are mainly distributed on shore, close to densely populated áreas, over North America, China, Japan and Europe [27]. Examples of seismic networks are the Southern California Seismic Network (SCSN), with more than 400 seismic stations, the China Seismic Networks, including a national network, several regional and local networks and mobile stations,

totalling about 1800 stations, the Japanese Seismic Networks, totalling almost 2000 stations, or the International Monitoring System (IMS), with about 200 stations. In spite of those numbers, the density of stations worldwide is still low. This fact, together with the reduced coverage across oceanic regions, results in a biased and poor spatially-sampled analysis of the global seismic activity. The cost of deployment and maintenance of a larger, denser and homogeneous cluster of seismological (traditional) sensors (including the oceans) poses a great economic challenge, making this solution practically unviable even for highly developed countries. Some of the recognized challenges for growing seismic networks are (i) the need of stringent (millisecond) synchronization between sensors, which is difficult to achieve for sensors offline, typically requiring a GPS clock (only available on surface); (ii) the reliability and cost of data transmission in real time and (iii) the individual power supply, battery life and maintenance of each sensor.

Distributed acoustic sensing is an emerging technology with enormous prospects in a myriad of scientific and technological areas, capable of detecting vibrations, strain and temperature variations along the length of an optical fiber (typically of tens of km, limited by attenuation and nonlinearity of fibers). For this purpose, a single interrogation unit placed at one end of the fiber is required, typically composed of optical and relatively low frequency (< 1 GHz) electro-optical components. Compared to traditional seismographs, DAS technology allows for a significant increment in the spatial information that can be obtained from a seismic event. Thus, while traditional monitoring devices are commonly placed separated by many kilometers (typically a few tens of kilometers, or eventually more densely placed only in specific areas), DAS systems allow for the monitoring of seismic activity with a spatial sampling of only a few meters. This represents a massive increment (e.g. about three orders of magnitude) in the spatial sampling and spatial information that can be obtained by DAS technology, and brings a completely different paradigm in seismic monitoring, allowing specialists to have an entirely new dimension to analyse and monitor the propagation of earthquakes. This attribute, along with the extensive coverage of optical fiber around the Earth surface (see Fig. *2*), assures an adequate platform for seismological tomography analyses. Besides, individual point sensors within the fiber are intrinsically synchronized, since all points are interrogated with the same unit. Distributed optical fiber sensors represent an inexpensive solution due to their long lifespan and their intrinsic low cost per monitoring point when dealing with long distances. Another important advantage of DAS (and DFOS in general) is their capacity to perform remote sensing, allowing the interrogation unit to to be kept in safe place away from harsh or hardly accessible locations and providing minimal intrusiveness in their deployment. This is particularly interesting for subsea ground motion monitoring, as it prevents expensive maintenance actions or power supply and reduces the risk of equipment damage.
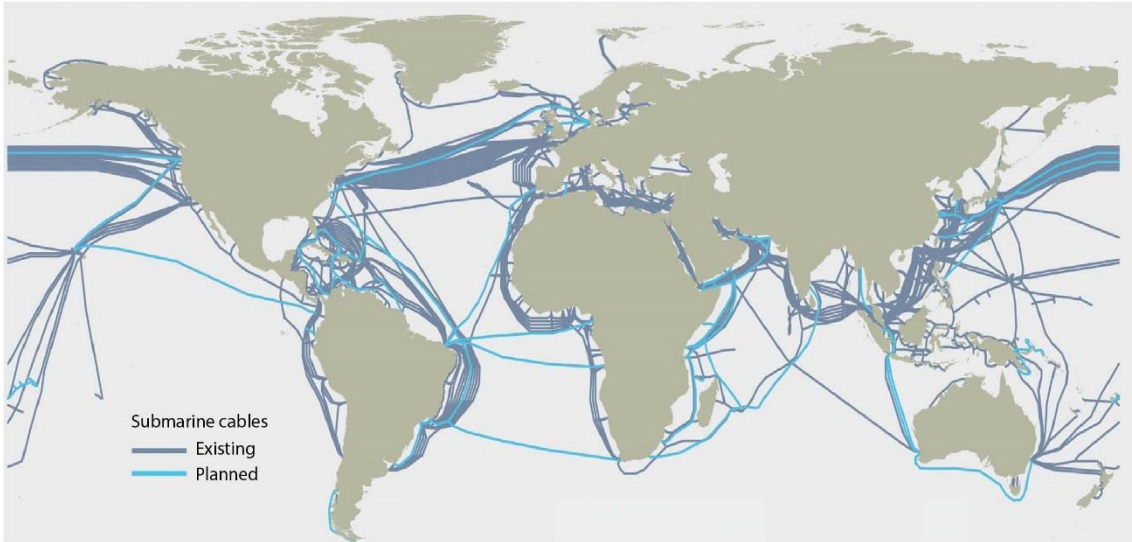
Fig. 2. (Extracted from Ref. [29]). Existing and planned submarine telecommunication fiber network. This infrastructure could be readily leveraged to acquire seismic information worldwide under the sea, where traditional seismographs are extremely scarce due to their elevated costs.

The huge amount of information obtained by the dense spatio-temporal DAS data can be indeed smartly used to improve the monitoring accuracy and to explore new methods for processing and analyse earthquake propagation. In this regards, disruptive signal processing approaches based on artificial intelligence, acoustic beamforming and multidimensional processing can be exploited, thus providing information that cannot be extracted using traditional seismic point sensors. Considering that the features of DAS data are very different compared to the one obtained by traditional seismic sensors (e.g. in terms of multidimensionality, noise level, sensitivity and precision), novel signal processing approaches have to be developed to extract much more meaningful and precise information. For instance, measuring the spatial distribution of seismic waves with metric spatial resolution can open up novel approaches to reliably measure propagation speed and dispersion curves of the seismic event. This will be essential for the development of modern and smart earthquake early warning systems in a near future. Indeed the potential use of the multidimensional features of the DAS data (e.g. distance, time, frequency, and wavenumber, and many others derived from domain transformation methods) represents a relevant advantage of this technology with respect to traditional sensors, which cannot benefit from the spatial information due to the extremely poor spatial density of the retrieved seismic data. This will be made evident in the results shown in Section 3.

2.2 STATE OF THE ART OF DAS

Distributed acoustic sensing relies on the elastic Rayleigh scattering generated in the sensing optical fiber. In particular, when a pulse of coherent light is launched into the sensing fiber, it experiences scattering due to the small inhomogeneities present in the fiber, which act as randomly-distributed partially-reflecting mirrors, as shown in Fig. 3. Any vibro-acoustic disturbance along the length of the optical fiber modifies the reflective characteristics of those mirrors, affecting the fiber signature. Eventually, the duration and exact location (within the attainable spatial resolution) of the perturbation can be readily extracted from the received backscattering trace. If the perturbation magnitude is to be quantified, more sophisticated strategies have to be followed. Note that the direct measurement of Rayleigh intensity trace along the fiber is normally an unreliable approach to quantify the magnitude of the perturbation, essentially due to the nonlinear (and non-monotonic) dependence of the Rayleigh intensity on

5

the strain induced over the sensing fiber. Nevertheless, two common techniques are typically employed to reliably quantify external perturbations: (i) the use of coherent detection of the optical field trace along with the extraction and analysis of the optical phase of the Rayleigh backscattered light [30–33], and (ii) the use of a chirped probe pulse along with direct detection of the Rayleigh intensity [34,35]. Note that another interrogation technique based on the use of a laser frequency scanning [7] is also widely used in Rayleigh-based distributed sensors to quantify the perturbation; however, its implementation imposes long measurement times, impeding true acoustic sensing operation.

Nowadays, commercial equipment can be found implementing Rayleigh-based DAS based on either coherent detection or chirped-pulses, although the latter has only been commercialized very recently. For this reason, to date most of the reported results on the use of DAS systems applied to seismic applications (Section 2.3) have been based on coherent detection and optical phase recovery.

In the remainder of this section, we review the technology and performance of the two main types of DAS.
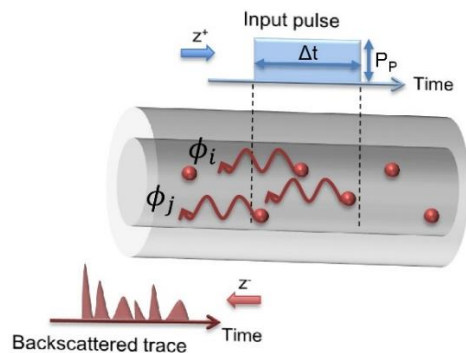

Fig. 3. Phase-sensitive optical time-domain reflectometry. Small inhomogeneities along the fiber structure behave as partially reflecting mirrors. The counterpropagating backscattered light that remains confined in the fiber interferes coherently upon reception, forming the optical trace that provides information about perturbations around the fiber.

2.2.1   Coherent-detection-based DAS

Any strain or temperature perturbation affecting the optical fiber produces linearly proportional variations in the phase of the backscattered trace, enabling quantification of such perturbation. The straightforward solution to acquire the trace optical phase is to coherently detect the trace at the receiver, either using heterodyne or homodyne detection [30,31]. Besides quantifying the perturbation, the optical phase of the received trace yields valuable information that can be exploited in many forms. Indeed, acquiring the optical phase has benefited the emergence of techniques aimed at increasing the measurement resolution and/or the energy efficiency, among which optical pulse compression [36] or pulse coding [37–39] stand out. In those techniques, the phase is to be detected to apply the corresponding matching filters to the received optical trace in the digital domain, aimed at recovering the perturbation information. Typically, the application of these methods has improved the spatial resolution of the measurement in about two orders or magnitude with respect to the transmission of a transform limited probe pulse.

However, the application of coherent detection in DAS systems entails several difficulties. The most detrimental problem of this approach is caused by the signal fading prompted by the interference of Rayleigh backscattered light. In regions where the optical signal fades, no reliable measurement of the optical phase can be performed (as illustrated in Fig. 4). This fact, together

with noise-induced instabilities in the phase unwrapping process and the intrinsic laser phase noise, deteriorates the accuracy of the sensor, even impeding its operation in numerous positions along the fiber [40]. Note that to reduce the impact of the laser phase noise in the trace phase determination, highly coherent lasers (i.e., with very narrow linewidth) are desired, substantially increasing the system cost. In addition, the backscattered light follows a random polarization, imposing the need for costly polarization diversity detectors [32]. To avoid the sensitivity fading problem, a receiver based on direct detection of the outputs of a Mach-Zehnder interferometer (MZI) followed by a 3x3 optical coupler has been used [33]. Yet, using an MZI at the receiver requires thermal and mechanical stabilization. Besides, a very precise coupler and three identical photodetectors are required for proper operation. These shortcomings hinder the application of this system beyond tests under laboratory conditions. A method that emulates the 3x3 coupler but employing a single photodetector has been demonstrated [41], which is based on three pairs of optical pulses phase-modulated to have a relative phase-shift of 0, $2\pi/3$ and $-2\pi/3$. With the use of a single pair of pulses, other methods have also been proposed for quantitative perturbation demodulation with no need for coherent detection [42]. However, the two latter methods require the perturbation to be narrower than the delay between pulses, and rely on intricate procedures that not only increase the measurement time (making them unsuitable for acoustic sensing), but also obstruct their application in real field test experiments.

It is important to notice that variations in the phase accumulate from the point of occurrence until the end of the fiber. Hence, a differentiation process is generally required to obtain a true measurement of the perturbation magnitude [43] . This process, with similar effects than a high-pass filter, further increases the detrimental effect of phase noise.

In spite of all the efforts to determine the trace optical phase avoiding the detrimental effects of coherent detection, to date phase detection is the approach included in most of commercially available DAS. While the use of signal post-processing can mitigate the effect of fading points [44], owing to their statistical nature, these algorithms may not be linear and/or predictable. The use of such algorithms therefore adds complexity, as artifacts may be introduced and/or relevant features removed. By accessing the raw signal, the danger of an additional layer that can tamper with the original signal is removed. This is particularly relevant for the detection of single events, which do not present a well defined statistical pattern.
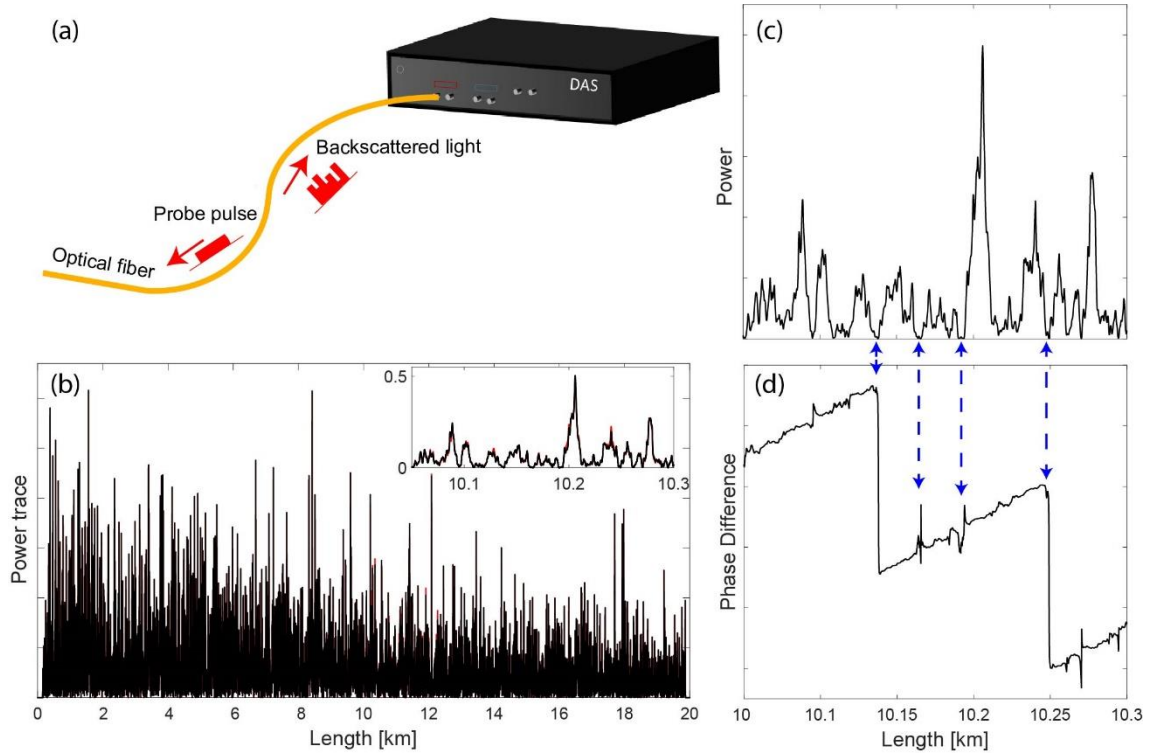
Fig. 4. (a) Principle of operation of DAS; a probe pulse travels along an optical fiber and the Rayleigh backscattered light that returns to the interrogator unit is photodetected and recorded (simulation). (b) Example of two consecutive photodetected power traces, obtained from a 20 km-long fiber, in which a 2 km-long uniform perturbation has occurred around the 11 km. Inset shows a zoom of the perturbed region. (c) and (d) show one power trace and the phase difference between the traces of (b). It can be seen how at locations where the trace fades, the measurement of phase is incorrect or even the phase reference can be lost. When the perturbation is non-uniform and unknown, those sensing points are inoperative.

2.2.2 Chirped-pulsed DAS

Few years ago, a novel technique exploiting the spectral properties of DAS was formalized and demonstrated [34]. This method, termed as chirped-pulse DAS, shifts the instantaneous frequency of a probe pulse along its width, producing a linear chirp. The propagation of a sufficiently high chirped pulse over the fiber induces a wavelength-to-time mapping on the backscattered trace [45]. A perturbation occurred nearby a fiber induces a proportional shift in wavelength of the backscattered trace locally at the perturbation position. Hence, the wavelength shifts caused by perturbations are translated to the time domain, producing proportional local temporal shifts in the received trace (see Fig. *5* for a visual representation of this principle). This difference in the principle of operation of DAS interrogation significantly alters the performance of the sensors, offering valuable advantages over all the above-mentioned schemes. In chirped-pulse DAS, quantification of the ongoing perturbation is attained by a simple time delay estimation process over the directly detected trace. Specifically, the time delay is measured via correlations between a reference trace and the subsequently received traces over moving windows of width similar to that of the probe pulse [46]. This behavior is one of the most distinctive features of chirped-pulse DAS, as it avoids the need for coherent detection or frequency sweeping strategies and associate shortcomings. In particular, chirped-pulse DAS shows neither polarization fading nor sensitivity fading associated to loss of phase reference in locations with low trace intensity [47]. In coherent detection-based DAS, this sensitivity fading critically affects the soundness of the sensor system. Instead, chirped-pulse DAS presents a steady sensitivity not affected by the power fading of the detected trace, leading to a quasi-deterministic acoustic SNR along the fiber length. Additional analyses on this implementation have revealed its capacity to

compensate for first-order laser phase noise, allowing a significantly relaxation of the coherence of the source (being still higher than the pulse width) while keeping a satisfactory level of SNR [48]. Besides, by reducing the correlation sampling error via interpolation processes, a record strain sensitivity for a DFOS has been demonstrated using this technique (in the pε/√Hz range) [46], still maintaining the spatial resolution and bandwidth of traditional DAS [47]. All the mentioned benefits of this novel DAS scheme has positioned it as a reference technique in many industrial and scientific areas in a very short time span. The interested reader can find a thorough review of chirped-pulse DAS technology in [35].
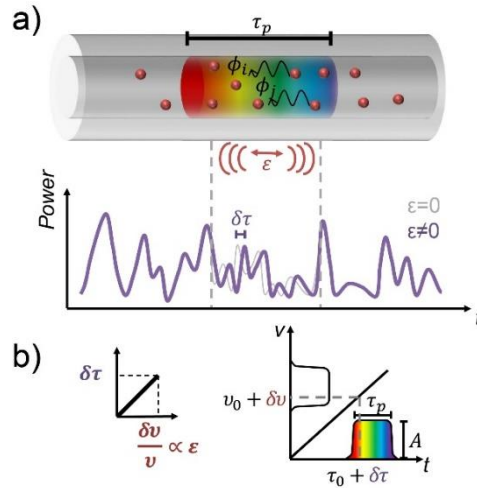

Fig. 5. Principle of operation of chirped-pulse DAS; a) a linearly-chirped pulse propagates through the fiber. Any strain perturbation on the fiber produces proportional, local temporal shifts in the generated trace; (b) The reason for this operation is the frequency-to-time mapping induced by a sufficiently high linear shift, which in turn produces a linear relationship between the trace temporal shift and the applied strain [34,46].

2.3 REVIEW OF USE OF DAS ARRAYS IN SEISMOLOGY

For several decades, the telecom sector has developed a ubiquitous network of optical fibers (onshore and offshore) that enables broadband connectivity all around the globe. Such an impressive arrangement of infrastructure and physical equipment over the Earth surface is currently employed exclusively (at least in the vast majority of cases) for telecommunication purposes. The re-purpose of this optical fiber network for distributed teleseism monitoring has been proposed in the last years, owing to the recent significant development of fiber-optic DAS [16–18]. The use of pre-existing telecommunication fibers could be leveraged to build large permanent or quasi-permanent seismic sensing network in an affordable and scalable fashion. On the other hand, it is possible to deploy a dense array of seismic sensors with adequate geometry or sensing properties by installing dedicated fiber cables for particular missions [19–22] (Fig. 6).

DAS deployments have been employed for decades for vertical seismic profiling applications, both onshore and offshore [49–52]. In these schemes, the optical fiber is installed in boreholes providing full well coverage, and it has been typically employed for exploration purposes and monitoring of reservoirs. However, their use has not been extended to other applications within geosciences until recently.

The first descriptions on the potential use of horizontal DAS for seismic monitoring date from 2013 [53]. Since then, several tests have been performed to examine the performance of horizontal DAS in earthquake detection and surface seismic monitoring [19,22,53,54]. Two main

challenges have been detected in the use of DAS technology. First, the fiber does not have broadside sensitivity, i.e., DAS can only record particle motion in the direction in which the fiber is oriented, having low sensitivity in detection of orthogonally oriented waves. To provide broadside sensitivity, approaches based on the use of helically wound fiber-optic cables have been proposed and examined [55,56]. Using this configuration, measurement of primary (P) body waves as a function of the angle of incidence have been reported, showing nearly angle independence [56]. The second challenge is the inaccuracy in the coordinates of DAS channels. The fiber provides the flight time of probe pulses along its length, but the cables may not (and typically do not) follow a straight line. In DAS-based seismic surveys using dedicated fibers, an approach based on tap tests along the cable has been demonstrated [22,57]. The tests employ instruments carrying a GPS unit to map coordinates for channels closest to the tap points, while interpolation is used to map the remaining channels. However, this solution may be hardly extrapolated to DAS networks using telecom fibers [58]. In those cases, a strategy based on application of machine learning using wave field features or ambient noise to map DAS geometry has been proposed [59].
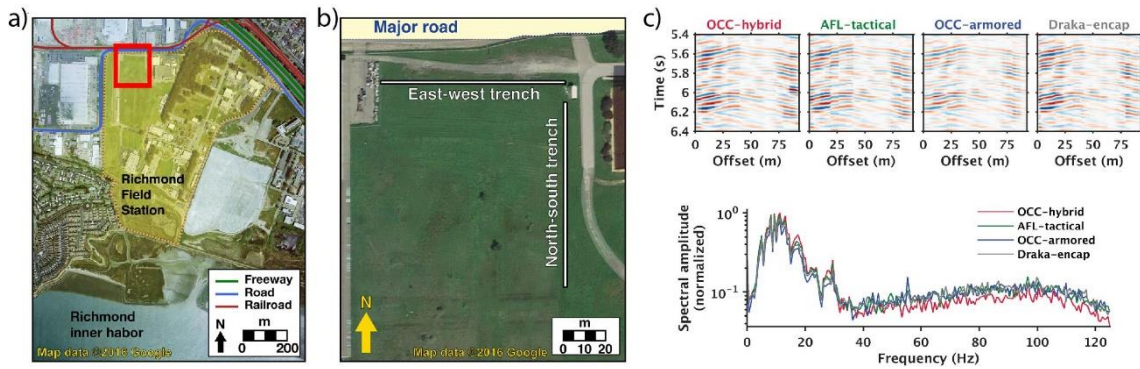

Fig. 6. (Extracted from [22]) (a) Location and (b) layout (L-shaped) of a DAS array specifically deployed for a particular field test in the Richmond, CA. (c) 1-s noise records (top) and mean spectral amplitudes for identical spatial and temporal windows using fibers with different packaging, showing minor influence in the DAS sensitivity.

In 2017, earthquake observations from different onshore quasi-linear DAS arrays distributed in a few locations in the United States were performed [19]. In all cases, DAS systems recorded different magnitude earthquakes with high waveform fidelity with respect to close seismometers. They also showed that the 2D (time vs. length) array response of DAS enables recording information that is not provided by conventional seismometers, such as the direction of the seismic energy. In a different field test that year, fiber with different packaging were tested, showing minor influence in the DAS sensitivity [22], as illustrated in Fig. 6(c). In 2018, the viability of using already-deployed fiber-optic telecommunication infrastructure for seismic monitoring was demonstrated for the first time [17]. Researchers occupied a 27 km section of dark fiber deployed in California and recorded ground motion activity along 7 months. An additional work exploiting the use of DAS combined with template matching processing has demonstrated the possibility of properly employing the large number of seismic channels in a DAS array to permit detection of small earthquakes even below the noise level [60]. However, this method relies on an updated catalog of predefined events, limiting its general use in the broad seismic tomography field. Certainly, as DAS arrays have been used just recently, a sound background of earthquake waveform templates and unsupervised machine learning-related approaches are yet to be developed, which surely will contribute to a broader detection and analysis of seismic patters (beyond those human labelled) [60–62].

Apart for seismicity monitoring, an appealing application of DAS arrays is that of sub-surface structure imaging. Typical spatial resolution of DAS (few meters) together with long ranges (tens of kilometers) allow conventional DAS to provide thousands of channels capable of sampling seismic waveforms without aliasing. This performance can be exploited to unveil structures of high interest in geophysics, such as fault zones or basin edges, aimed at extracting information about earthquake dynamics, ground shaking predictions and more. Traditionally, those observations have been achieved using temporary dense nodal seismic arrays [63,64]. However, DAS arrays may provide unparalleled performance while avoiding the shortcomings of deployment of large point seismic sensors, as described in Section 2.1. For this purpose, several field tests have been carried out to date, either employing active (using earthquake waveforms [16,65]) or passive methods (using ambient noise correlation or seismic noise such local traffic [17,21,22,58]), with very promising results. In all cases, a critical factor of success depends on the recognition of the cables geometry.

All the previously mentioned studies have been performed onshore using commercially available DAS technology based on coherent detection φ-OTDR. Solutions based on DAS using passive 3x3 coupler demodulation have been also proposed in the literature [54]. However, this approach has only been tested under non-realistic, well-controlled experimental conditions, since this receiver requires thermal and mechanical stabilization, hindering its application in field tests. Regarding ocean-bottom seismic monitoring, in [29], researchers reported the detection of earthquakes over terrestrial and submarine links with lengths of >500 km and a geographical distance from the earthquake epicenter ranging from 25 to 18,500 km. For this purpose, the used interrogator employed an ultralow expansion cavity-stabilized laser. Such a complex interrogator unit is costly and difficult to handle, limiting its escalation for real use around the globe. Besides, no distributed sensing can be realized using this approach, as the whole fiber is used as a single sensor. In the following Section, we show the first experimental demonstrations of the use of chirped-pulse DAS for monitoring tele-seismic activity, using both an ocean-bottom DAS and a DAS employing an already-deployed metropolitan telecom fiber. For the latter case, we present the optical configuration used as well as several signal processing algorithms employed for recovering seismic information from the acquired strain signals. We note that these waveforms are acquired in particularly noisy environments, but the earthquake waveforms could be extracted with moderately high fidelity thanks to the high spatial sampling provided by DAS arrays.

3 Seismic Monitoring in Noisy Environments using Chirped-pulse DAS

As mentioned in Section 2.1, a fundamental benefit of DAS systems is the intrinsic high spatial sampling offered by the optical fiber, capable of providing a strain sensing unit every few meters. This attribute allows the acquisition of spatio-temporal information of the recorded seismic events. The spatial dimension, not available when using a single seismograph or insufficiently sampled in conventional seismic arrays (due to the typically high distance between seismographs allocation, in the km range), enables a better discrimination of seismic events with respect to noise. As such, conventional seismographs can only discriminate events in the frequency domain. Hence, if noise is present at seismic frequencies, it will be considered as a seismic stimulus. When using a DAS, however, events can be discriminated in both frequency and wavenumber, which can be readily exploited for applying effective denoising strategies.

In this Section, we illustrate this important property through the detection of teleseisms in highly noise environments using a chirped-pulse DAS. In particular, we show the detection of an M8.2 earthquake occurred in August 2018 in Fiji through already deployed optical fibers. The earthquake was simultaneously detected in two different scenarios with identical interrogation units: an ocean-bottom fiber in Zeebrugge (Belgium) and a telecommunication fiber in Pasadena (CA, USA). The results obtained from the Belgium array have been recently published [66], where an analysis of subsea seismicity has been carried out. Here, we extend the results acquired from the fiber in Pasadena [67,68]. In both situations, the noise values in the raw recordings from an offshore shallow fiber and a densely-populated metropolitan area exceed (by several orders of magnitude) the seismic information. The absence of sensitivity fading in chirped-pulse DAS is particularly interesting in these cases, as it permits the application of rather simple array post-processing techniques since the raw data is processed as recorded, having all points along the fiber similar sensitivity/noise characteristics. Besides, chirped-pulse DAS has proven to have additional outstanding features compared to coherent detection-based schemes. Among them, we can highlight the high strain resolution for low spatial resolutions (reaching $p\varepsilon/\sqrt{Hz}$) [46], its robustness against laser phase noise [48], a higher reliability and dynamic range, as this technique is insensitive to trace fading points [47], measurement ranges capable of exceeding 100 km [35,69], and all this with a simpler and cost-efficient scheme based on direct detection [34]. These attributes may position chirped-pulse DAS technology as a critical sensing tool in future seismic telemetry systems.

3.1 Teleseisms Monitoring in a Metropolitan Area

Pasadena is a dense-populated metropolitan area at >9,000 km from the earthquake epicenter, where traffic and ambient noise amply surpasses the amplitude of seismic waves detected by the DAS. The experimental test is performed under real conditions with a simple, relatively low cost and high-performance interrogator unit. In what follows, we describe the employed interrogator unit, the measurement conditions and then we show the obtained results, prior and after the application of several signal-processing techniques. The outcome is compared with that obtained from a nearby seismometer, showing good correspondence in all cases.

3.1.1 Optical setup

The optical setup of the employed interrogator unit is very similar to that of a conventional DAS [34], and is shown in (Fig. 7 (b)). A coherent laser source (1 MHz-linewidth) is pulsed using a semiconductor optical amplifier (SOA) in order to supress the intra-band coherent noise [70]. The SOA is driven by square-like pulses generated using a signal generator. The pulses are 100 ns-width with a peak power of about 0.2 W and repetition rate of 2 kHz (corresponding to the acoustic sampling frequency). An electrical ramp modulates the current driver of the laser source in order to generate the linear chirp, inducing a total probe bandwidth of 500 MHz (resulting in an instantaneous frequency slope of 5 MHz/ns). An amplification stage composed of an erbium-doped fiber amplifier (EDFA) plus a band-pass filter (BPF) (aimed at reducing amplifier spontaneous emission (ASE)) follows the pulse generation arrangement. The resulting probe pulse is then launched to the sensing fiber through an optical circulator. The fiber is a ~26 km-long standard G-652 telecommunication fiber installed across the city of Pasadena, CA, as depicted in Fig. 7(c). Geometrically, it runs in three main sectors starting from the South Mudd building in Caltech, as shown in Fig. 7(a); first 2 km from East to West, followed by 4 km from South to North and lastly 5 km from West to East. Several fiber loops exist along the installation, increasing the total real fiber length, which includes a section of about 1 km of aerial cable that

introduces noise to the acquired signals. Distributed amplification using Raman scattering is applied to compensate for fiber losses and increase the SNR of the resulting trace [69]. The backscattered light received at the launching end of the fiber is additionally amplified via another amplification stage (EDFA + BPF) before photo-detection. The resulting signal is subsequently detected using a 0.5 GHz-bandwidth photo-detector and recorded via a 1 GS/s acquisition card.
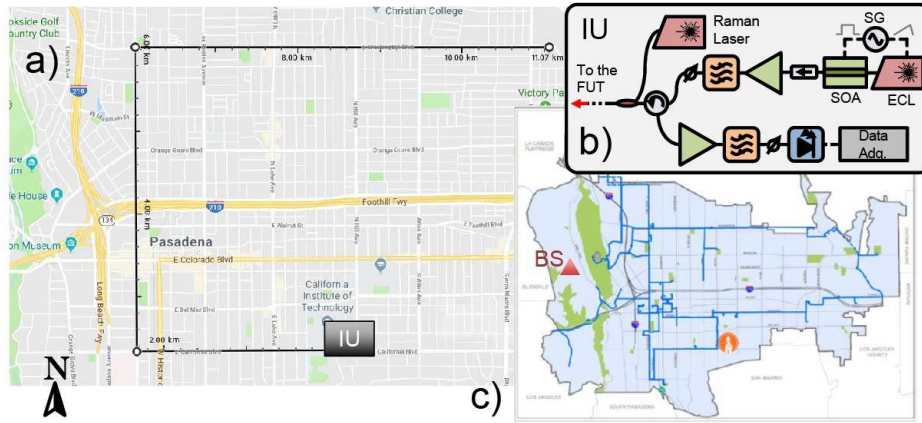

Fig. 7. a) Geometrical distribution of the sensing fiber. Seismic waves of the Fiji earthquake propagate mainly from West to East direction; b) Optical setup of the chirped-pulse DAS interrogator unit (IU). Dashed lines represent electrical path, solid lines represent optical path and the dotted line represents the connection to the fiber under test (FUT); c) Real fiber network array in Pasadena, showing several loops that contribute to increase the fiber length with respect to the geometrical distance (modified from Pasadena GIS – DoIT [71]). The approximate location of the broadband seismometer (BS) used as a reference is marked in this figure.

3.1.2   Measurement conditions

The spatial resolution (or gauge length) of the employed sensor is 10 m, as imposed by the probe pulse width. This is equivalent to having one seismometer placed every 10 m (this is commonly called channel spacing in seismology), measuring the average strain over a fiber length of 10 m. In total, there are 2592 measured channels (i.e., independent sensing points) over ~26 km of fiber installation. Each channel is initially sampled at 2 kHz (imposed by the pulse repetition rate) and later downsampled to 50 Hz in order to reduce the dataset size. A total recording time of 1 hour and 10 minutes (4200 s) is evaluated.

The sensing fiber monitoring the earthquake corresponds to an existing optical fiber already installed in Pasadena (CA, USA), at >9,000 km from the earthquake epicenter. A detailed description of the seismic wave propagation from the epicenter to the recording location is out of the scope of this work. However, by analysing the collected traces along the fiber geometrical distribution, it is clear that the seismic waves arrived at Pasadena mainly from West to East (W-E) direction. Recall that the optical fiber is sensitive to strain variations along the direction in which it is oriented, and hence the existence of perpendicular fiber sections in this arrangement provides information about the wave propagation direction. Consequently, in order to analyze the earthquake propagation, we process here only the last 5 km of fiber, corresponding the last section in W-E direction.

Fig. 8(a) shows the measured raw strain recorded during the occurrence of the Mw8.2 earthquake on August 19th 2018, between 00:13 and 01:23 UTC along the last 5 km of fiber. Fig. 8(b) presents a frequency-wavenumber (f-k) domain representation of the recorded set, which is obtained by the 2D Fast Fourier Transform (FFT) of the data shown in Fig. 8(a).
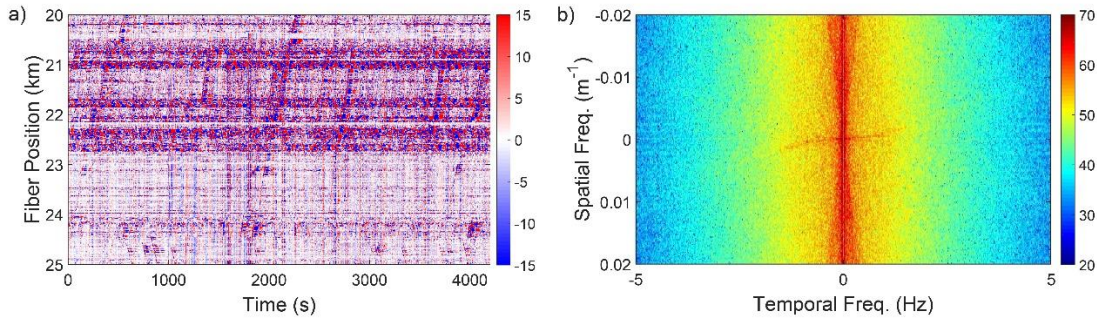
Fig. 8. (a) Strain recordings versus time and length obtained during the Fiji earthquake from a chirped-pulse DAS located in Pasadena, CA; (b) Frequency-wavenumber (f-k) representation of (a).

It is clearly visible from Fig. 8(a) that ambient acoustic noise (vehicles and nearby machinery) is significantly stronger than the seismic signals, which have nevertheless very characteristic features (i.e. the weak quasi-vertical lines appearing along the image). Note that the detected moving perturbations along the fiber produce a linear trail whose slope is proportional to its velocity. For example, it is very simple to recognize in the figure vehicles riding parallel to the fiber over considerable distances (2-3 km), which appear as straight lines with different orientations (i.e. different velocities). Seismic waves appear as quasi-vertical lines, as their velocity is extremely fast (in the order of km/s) compared to normal vehicles. Additional sources of acoustic noise are also evident in the trace, including the effects appearing in the loose fiber sections, which obviously remain always in the same position. Considering the extreme difference in frequency and wavenumber features of the seismic and ambient noise waves, it is possible to very clearly distinguish and isolate each type of feature in the frequency-wavenumber (f-k) domain (Fig. 8(b)). As it is visible, most of the energy appears at very low frequencies (<0.1 Hz), corresponding to thermal fluctuations appearing almost at all spatial wavelengths. Still, almost horizontal lines in the first and third quadrants of the Cartesian plane are distinguishable, showing long-wavelengths (i.e. low wavenumber) and frequencies up to ~1 Hz. These components correspond to seismic waves (with a velocity of ~750 m/s) propagating in the W-E direction (i.e., moving away from the fiber launching end). Hence, distinctive features of seismic waves are also well appreciable in the f-k domain.

3.1.3 Signal processing algorithms

Apart from target seismic waves, a DAS system detects any kind of vibro-acoustic perturbation befallen around the sensing fiber. The raw strain records from the DAS array in Fig. 8(a) show little coherence in the time domain, since ambient noise from traffic and other events affecting the environmental conditions are dominant. Indeed, the recorded strain amplitudes originated by environmental acoustic sources are more than one order of magnitude higher than the seismic waves to be detected. For this reason, it becomes important to implement digital signal processing approaches to eliminate the noise interfering with the seismic signal of interest, so that the earthquake signal could be clearly discriminated and retrieved from the rest of detected acoustic signals (which might contain additional useful information, but will be considered as noise for the purpose of this work).

The raw strain data measured by the DAS system can be arranged in a 2D matrix containing the measured strain vs time and space. This data structure can be seen as an image containing a useful signal in the spatio-temporal domain, being however corrupted by noise. As mentioned before, this noise does not only correspond to Gaussian additive noise introduced by the photo-electronic detection but also contains environmental acoustic signals that are of no interest for

14

the purposes of seismic detection. Due to the 2D features of the data, 1D and 2D signal processing methods can be applied to eliminate noise. In this case, two different signal-denoising methods are tested to retrieve the seismic information. In particular, the particularities and suitability of one 2D linear band-pass filtering process and one 1D nonlinear denoising algorithm based on adaptive filtering will be presented here below.

Once suitable denoising processing algorithms are applied to the raw data, the processed signals are compared to the signal recorded by a nearby broadband seismometer (BS) in the West-East direction. This reference seismic trace is denoted as BHE trace, where B stands for broadband seismometer, H indicates that the seismometer measures particle motion and E refers to the wave direction of propagation, namely West-East. Given the quasi-linear geometry of the selected section of sensing fiber, neither corrective algorithms to compensate cable turns nor adjustment of the exact seismic propagation angle have been applied, resulting in a slight smearing of energy along the wavenumber axis. For an exact comparison between DAS and BS data, the raw strain amplitude measured by the DAS system should be rigorously converted to particle velocity records (BS recordings). However, it can be assumed that the main spectral features are essentially comparable in both types of instruments (assuming reasonably low particle velocity dispersion over the considered frequencies), and the error in the comparison remains relatively small if we do not perform any conversion. Thus, we directly compare strain (DAS measurement) with particle velocity (BS measurement) to roughly check the curve fitting between instrument recordings [72].

3.1.3.1 *Two-dimensional linear band-pass filtering*

In general, when the sampling frequency of a signal exceeds considerably the useful signal bandwidth and the measurement is affected by large levels of noise, linear low-pass and band-pass filters offer an excellent possibility to reduce noise and improve the signal-to-noise ratio of the desired signal of interest. Given the sampling rate of the acquisition system (pulse repetition rate of 2 kHz), large part of the 2D digital band contains noise; being of interest only the spectral regions with temporal frequencies below 1 Hz and spatial frequencies below 10^{-3} m^{-1} (i.e. period over 1 km), as shown in Fig. 8. The computed 2D FFT of the recorded data (f-k domain representation, see Fig. 8 (b) is employed to establish the transition bands of the filter. In this case, we have employed a 2D rectangular band-pass filter that maintains the temporal frequencies ranging from 0.02 Hz to 1 Hz, and the spatial frequencies ranging from 0 to $2 \cdot 10^{-4}$ m^{-1}. Note that instead of a low-pass filter, a band-pass filter has been here used to remove temporal frequencies below 0.02 Hz, and thus eliminate the temperature drifts affecting consecutive measurement. The filter only includes passbands in the quadrants 1 and 3 of the Cartesian plane, corresponding to moving targets going in the W-E direction. Fig. 9(a) shows the trace channels resulting from the application of the described filter.
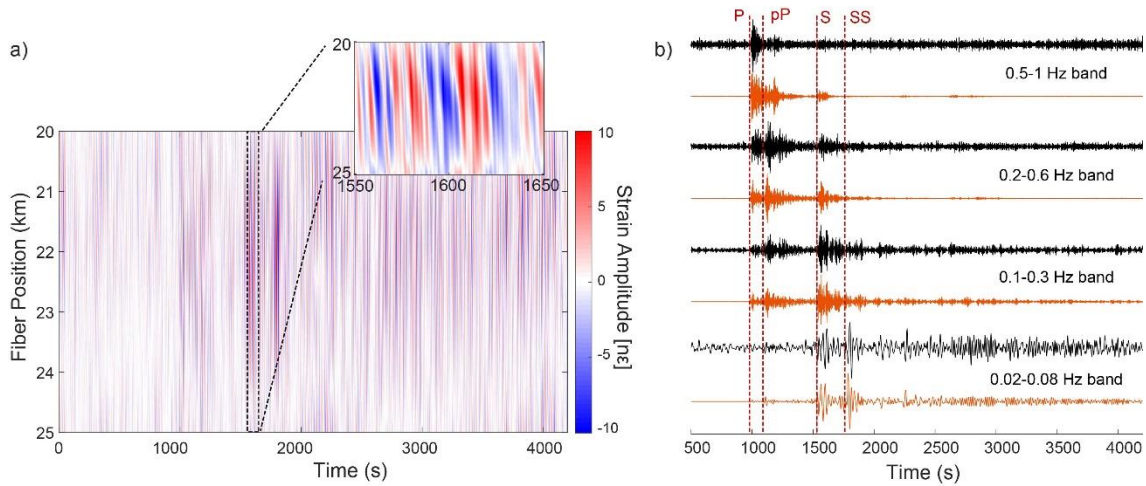
Fig. 9. (a) Strain recordings versus time and length after 2D linear filtering. Only seismic waves propagating from West to East detection have been maintained; (b) Comparison of stacked DAS traces (black line) and traces obtained by nearby seismometer (orange line) at the W-E direction, filtered to various bands between 0.02 Hz and 1 Hz and normalized to particle velocity.

As it can be seen from the outcome (Fig. 9(a)), most of the noise components have been eliminated by the 2D BPF. The resulting signal after filtering is compared with the BHE trace of a nearby BS. Fig. 9 (b) shows the comparative normalized results of both sensors for different spectral bands. It can be seen how at frequencies >0.2 Hz, the primary waves (i.e., P wave, which is a seismic wave that has propagated through the mantle and outer core of the Earth, and pP, which is a surface reflection of a P wave) are dominant. Secondary waves (i.e., S and sS) appear several minutes later than primary waves and present frequencies <0.2 Hz. At lower frequencies (two bottom lines of Fig. 9 (b)), the curves recorded at >2600 s by the DAS and BS present similar content (the overlapped curves match) but with different amplitudes. This is because DAS and BS measure different parameters: while DAS measures strain variations along the gauge length (~10 m), BS measures particles velocity at a single point. Still, as it can be observed from the figure, chirped-pulse DAS strain measurements follow very similar patterns compared to broadband seismograph recordings, assuring the reliability of the fiber sensor. The good quality of the results, together with their low computational cost makes 2D linear filtering a highly suitable solution for this particular application.

3.1.3.2 *One dimensional adaptive filtering*

The previous filtering method does not take into account the variations of the signal bandwidth over time, resulting in a time-invariant filter that only considers the mean features of the spectrum. A different strategy is to use adaptive filtering, in which the filter bandwidth is modified over time, in order to match the time evolution of the signal bandwidth.

The structure of an adaptive filter contains adjustable parameters, whose values change over time following a procedure of adaptation based on the features of the signal. The filter structure can be constructed based on a finite impulse response (FIR) filter or infinite impulse response (IIR), while the adaptation can be carried out following, for instance, a least mean square (LMS) or recursive least square (RLS) algorithm. In this case, DAS data has been filtered using a FIR filter, since this kind of structure demonstrates to have better stability than IIR filters, while adjusting the coefficients of FIR filters is usually simpler than adjusting the coefficients of IIR filters.

On the other hand, the adaptive procedure uses a reference signal that is compared to the input signal to be filtered. In this case, the signal measured by the seismograph can be used as a reference signal to estimate the bandwidth variation of the signal over time. A LMS adaptive procedure is used to adjust the parameters of the filter in order to minimize the difference between these two signals and to maximize the signal-to-noise ratio of the filter output. Note that, however, in case no reference signal is available, blind adaptation algorithms can be used. This is indeed an interesting approach for further research, however, a thorough investigation on this subject is out of the scope of this paper. Here, the concept of adaptive filtering is tested and proved based on the spectral changes of the seismic signal monitored by the available BS placed near the sensing fiber. A comparison of the post-processed DAS traces and the signal recorded by the seismometer for different spectral bands is shown in Fig. 10, *demonstrating an excellent match in all cases, and reduced noise level compared* with the linear filtering process.
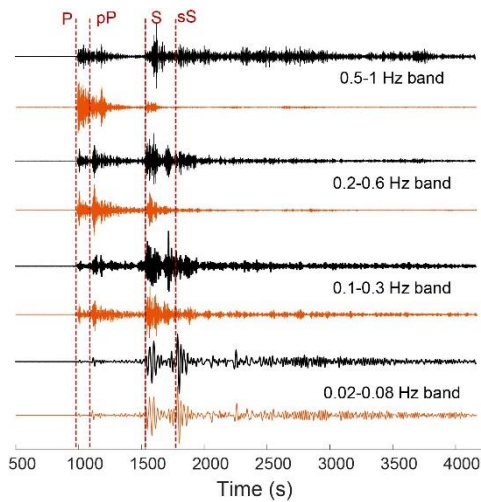

Fig. 10. Comparison of stacked DAS traces (black line) and traces obtained by nearby seismometer (orange line) at the W-E direction, filtered to various bands between 0.02 Hz and 1 Hz and normalized to particle velocity.

3.1.4 Results and comparison of different denoising approaches

Figure 11 summarizes the results of the applied denoising techniques by showing the spectral evolution over time for the monitored seismic activity. In particular, Fig. 11(a) shows the spectrogram of the seismic wave measured by the seismometer placed next to the sensing fiber and used as a reference for comparison with respect to the DAS data. Fig. 11(b) shows the spectrogram of the DAS data obtained after the previously described linear 2D band-pass filtering. The figure demonstrates the great similarity between the data obtained by the DAS sensor and the seismometer, showing similar time-frequency dynamics in both cases. An alternative procedure for more efficient noise removal is shown in Fig. 11(c), providing the outcome of an adaptive LMS filter. In this case, the filter bandwidth changes over time following the seismometer signal as a reference for estimating the bandwidth evolution. Compared to the band-pass filter, adaptive filtering maximizes the SNR of the measurements due to the possibility to adapt the filter bandwidth over time, thus enabling the efficient elimination of both detection noise and acoustic (background noise) interference.

Besides, it is important to highlight that other nonlinear signal denoising algorithms have also been evaluated, such as wavelet denoising methods based on 1D and 2D discrete wavelet transform (DWT). However, these methods did not bring major benefits in this particular case when compared to 2D linear band-pass filtering. This is because the measured earthquake has spectral components in the entire frequency range below 1 Hz, where wavelet thresholding does

not have any significant effect. Nevertheless, wavelet denoising could be still further investigated under different earthquake scenarios, since the filtering capabilities of the method highly depend on the spectral content of the earthquake energy and the features of wave propagation.
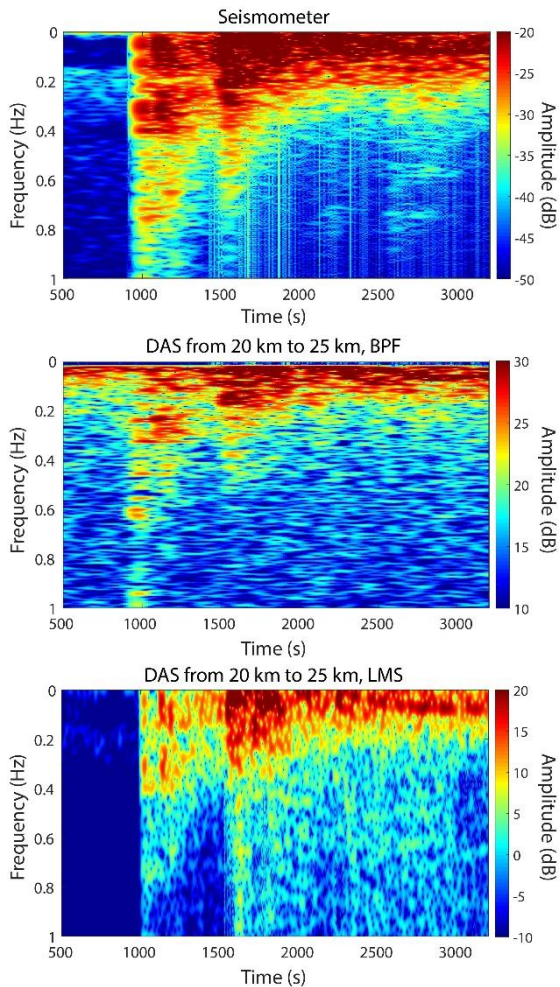

Fig. 11. (a) Spectrogram of seismic signal measured by a reference seismograph. (b) Spectrogram of DAS data denoised by a 2D linear band-pass filter. (c) Spectrogram of DAS data denoised with a 1D adaptive LMS filter.

3.2 OCEAN-BOTTOM SEISMIC ANALYSIS

A chirped-pulse DAS identical to the one described in Section 3.1.1 interrogated a 42 km optical fiber deployed to monitor a power cable from an offshore wind farm close to the city of Zeebrugge. The fiber is almost perpendicular to the shore, reaching almost 33 m of depth (see Fig. 12(a)). Such a shallow fiber is highly exposed to surface noise, such as ocean waves or ship-induced noise. The fiber is almost straight, with minor bends every 10 km that have been not compensated after data acquisition, resulting in slight smearing of energy along the wavenumber axis. The spatial resolution is also 10 m, totalling 4192 channels recording seismic information [66].

In this case, both seismic and oceanic information were extracted from ambient noise by using a methodology similar to the one exposed in Section 3.1.3.1, i.e., the different waves of interest are identified and separated based on their characteristics phase velocities ($v_p = f/k$), by simply applying 2D linear BPF on the f-k representation of the acquired data. Three different kind of processes were analyzed from 4200 s of acquisition. The fist process was microseism generation,

which is seismic noise with particular features typically recorded by seismographs, which has been long attributed to ocean wave sources. Microseism generation is a subject of continued research, and can be directly detected by chirped-pulse DAS acquisitions, as it has been demonstrated by the acquisition of ocean surface waves and Scholte waves. Ocean surface waves are excited by wind-sea interaction. Those waves could be found in the four quadrants of the f-k representation (i.e, propagating both seawards and landwards) between <0.01 and 0.3 Hz. The dispersion relation of measured waves perfectly matched the theoretically expected dispersion expression. Scholte waves, on the other hand, are seismic waves propagating faster than 300 m/s at frequencies >0.3 Hz, and also showed consistency with the expected dispersion relation of Scholte waves along the sediment-water interface. The second analyzed process was about ocean waves and currents; spatial variations in the intensity of landward-propagating versus seaward-propagating ocean surface gravity waves could be distinguished from the f-k spectra along different segments of the cable, proving the potential of ocean-bottom DAS for investigations in physical oceanography. Finally, the M8.2 Fiji earthquake was also detected from this location in Belgium (more than 16,300 km away from the epicenter) (see Fig. 12(b)) [66]. Note that the two former processes (namely, microseisms and ocean waves) have a noise nature for teleseisms detection. As shown in Fig. 12(d), teleseisms are correlated with ocean waves in frequency, and with microseisms in wavelength. Nevertheless, the spatio-temporal information provided by DAS arrays enables a proper discrimination of teleseisms from both sources of noise. Figure 12(e) and (f) show the comparative between the spectrogram of the teleseism waves acquired by the DAS (stacked along 5 km, in a processing procedure similar to the one realized in Section 3.1.4) and by a nearby seismometer. Figure 12 (g) shows the stacked traces along 5 km filtered to various bands between 0.02 and 1 Hz, compared to amplitude-normalized particle velocity from acquired by the nearby seismometer (similar analysis than the one presented in Section 3.1.3.1). The presented and analyzed observations of seismic and ocean waves on an ocean-bottom DAS array have demonstrated that chirped-pulse DAS can offer high value in seismographic and oceanographic data products.
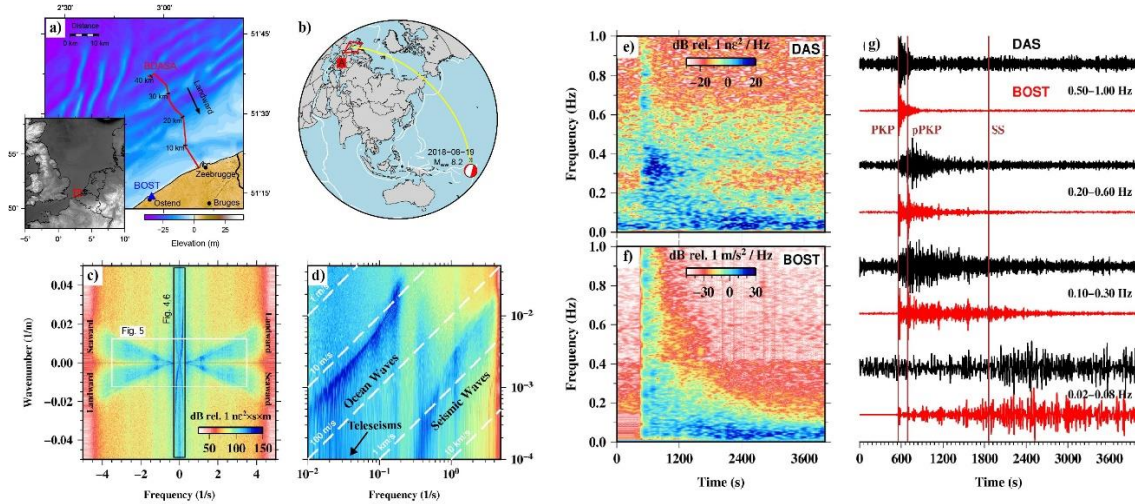

Fig. 12. (Extracted from Ref. [66]) (a) Location of the DAS array installed in Zeebrugge (Belgium). (b) World map showing the locations of the DAS array and the recorded M8.2 Fiji earthquake. (c) Raw f-k power spectrum of 1 hour of DAS strain acquired along the whole fiber length. (d) Zoom of the first quadrant of (c), corresponding to landward-propagating waves), showing waves at different phase velocities, enabling identification of ocean and seismic waves. (e) Spectrogram of PSD over time for the f-k filtered and stacked DAS beam trace (black in (g)). (f) Spectrogram of PSD over time for the data acquired by a nearby seismometer (BOST, red in (g)), showing the same major features than in (e). (f) Stacked DAS beam trace (black) filtered to various bands between 0.02 and 1 Hz compared with amplitude-normalized particle velocity from broadband station BOST rotated into the mean azimuth of the DAS array (red).

4 FUTURE LINES OF WORK

The re-purpose of the already-installed telecommunication optical fiber network for distributed teleseismic monitoring stands up as a promising solution for the recording of ubiquitous ground motion events for seismic tomography studies. Preliminary research on the use of DAS methods to convert the optical fiber into a dense array of seismometers have been recently reported, generally using dedicated fiber or fiber installed in low noise environments. Generally, the DAS systems usually employed in seismography (i.e., those based on coherent detection schemes) are typically 1-2 order of magnitude less sensitive than currently available geophones. In spite of this, DAS measurement provides important advantages over traditional geophones, such as a high spatial resolution (in the meter scale), unlimited deployment duration and ubiquity all around the globe with minimal deployment cost. The high spatial and temporal sampling associated to the attained resolution and acoustic bandwidth (e.g., 0.1 m^{-1} and 2 kHz in the presented proof-of-concept experiment) can be readily exploited for a more effective data processing, aimed at reducing ambient noise. This attribute redresses the worse performance of DAS (in terms of SNR) compared with traditional seismology sensors. In this work, a recently introduced DAS method based on the use of probe chirped pulses has been tested for teleseismic monitoring in highly noisy environments. Pre-installed fibers from (i) the telecommunication network of a densely populated area and (ii) an ocean-bottom power cable monitoring system have been used, providing encouraging results over realistic environments. Chirped-pulse DAS has proven capable to achieve record sensitivities for a distributed sensor [46] (particularly for low spatial resolution settings, as required for seismology), showing promising possibilities for improved capabilities in the detection and quantification of seismic activity.

A crucial feature of chirped-pulse DAS is the uniform acoustic sensitivity they provide along the entire fiber length, provided that there is a healthy level of optical SNR [47]. This has a particular impact on the signal processing algorithms subsequently applied to the recorded data. Specifically, the raw data as received can be processed using the selected processing method, having all points similar level of noise (similar sensitivity) with no need for applying previous smoothing or corrective algorithms. In particular, in this paper we have evaluated the use of one-dimensional and two-dimensional denoising algorithms. Results obtained by 2D linear band-pass filtering turn out to give fairly good outcomes as compared with those obtained by a reference seismometer; however, the use of a linear adaptive filter allows for reducing noise following the evolution of the signal bandwidth over time.

The ubiquity of optical fiber around the Earth surface and the high sensitivity attainable show promise to eventually convert the worldwide optical fiber infrastructure into a new generation of seismic instrumentation covering the entire planet.

4.1 CHALLENGES OF THE TECHNOLOGY

In spite of the large steps forward achieved by DAS technology within the field of seismic monitoring, there are important technological challenges that must be resolved before DAS systems become completely operative for this application on a global scale. First of all, DAS systems are not currently implementable on transoceanic fibers covering their whole length. Although operation of DAS well over 100 km range can be envisioned using a combination of distributed amplification and probe pulse modulation techniques [35,69,73,74], their implementation on the existing telecom fiber installation remains a challenge. Still, tests have been already performed demonstrating the capability of using bidirectional optical repeaters to break the

current range limits of distributed sensing technology [75]. Hence, the compatibility of this technology with optical links operating under water is patent, as optical repeaters exist typically every 80 km approximately. Another major difficulty of DAS in seismology is its one-directional sensitivity. As commented above, a solution based on helically wound optical fibers has been already proven [56], offering 3D sensing of seismic waves. An additional issue to be discussed is the infrastructure allocation plan. A potential way to employ the currently existing optical fiber network with minimal intrusion is through the use of dark fibers, which are unemployed fibers deployed in case of damage of operative fibers and in foresight of future increasing needs of information data rate. Dark fibers could be readily employed as sensors, as it is the case presented in this work. Alternatively, new methodologies to employ operative fibers via multiplexing solutions or even directly using information channels could be explored [37].

More related to the particularities of chirped-pulse DAS technology, long-term (> 24h) stability must be analyzed in depth in order to validate the viability of the technology for the monitoring of Earth tides. To date, evaluation of chirped-pulse DAS stability has been only performed for temperature variations, attaining < 0.1°C (precision of the used thermometer) accumulated error over several hours [34], which would correspond to < 1,000 nε of strain accumulated error. Besides, the majority of applications of chirped-pulse DAS have pushed the system optimization in terms of noise for frequencies well above those of interest for seismology (< 1 Hz). Techniques to reduce low frequency noise (i.e., in the 0.01-10 Hz range) in chirped-pulse DAS, which can be attributed to the presence of large errors [76] or polarization noise, are yet to be proposed and validated.

4.2 FUTURE OF DAS IN SEISMOLOGY

Distributed acoustic sensing has just recently started to be an active actor in the geophysical field, and hence only preliminary data acquisition and comparative analysis of recordings with those from well-established equipment have been performed to date. Consequently, there exists a myriad of applications and placements to be explored, which could also benefit from the unique strengths of DAS.

Amongst applications, DAS systems could be applied to extract fundamental information from the monitoring of active volcanoes, slow-moving landslides or even could be installed in seismic inactive regions (currently poorly instrumented) for structure imaging, leveraging their low deployment and maintenance cost. Regarding new placements in which DAS could provide relevant information, to date scarce tests have been done in oceanic environments [29,66,77], in spite of the fact that the distribution of earthquakes is mostly restrained near plate boundaries. Currently, most of the current seismograph networks are placed onshore. Hence, the widespread use of sub-sea DAS opens a host of new possibilities for seismic exploration for DAS arrays. Ocean-bottom DAS could permit the extraction of critical information in geophysics, from Earth tomographic images to the understanding of large earthquakes rupture (typically occurring in submarine settings).

DAS systems could be also of great utility for the monitoring of glacier seismology. The remoteness and harsh environment of many glaciology research regions make the deployment and maintenance of seismic stations extremely expensive. However, DAS systems are excellent candidates to provide a dense array of seismic stations, robust against environmental conditions in glaciers, having the power consumption and data storage at the end of a fiber in a safe location. The sensing performance of DAS could allow the study of a wide range of glacier-related processes, which could be combined or complemented with DAS deployment in

boreholds (e.g., by hot water drilling) to provide unique datasets of subglacier or englacier seismic events.

Finally, DAS systems can be also thought to be part of seismological analysis in planetary missions. To date, just few stations have been included in certain missions (e.g., Mars Insight, Apollo). However, knowing the internal structures of other terrestrial planets or the Moon could be of immense interest for geologists, even to better understand the Earth's formation and evolution. Similarly to the glacier case, the sensing optical fibers are robust to harsh environments, immune to electromagnetic interference, while the interrogator unit may be placed in a better controlled, safe place (e.g., a lander). Still, DAS systems and most of conventional optical fibers are not yet space-proof, and further evolution in these systems may be needed before DAS systems are ready to be part of planetary missions.

5 ACKNOWLEDGEMENTS AND FUNDING

6 REFERENCES

[1] K.T. V. Grattan and B.T. Meggitt, *Optical Fiber Sensor Technology: Fundamentals* (Springer US, 2000).

[2] A. Rogers, Meas. Sci. Technol. **10**, R75 (1999).

[3] A.H. Hartog, *An Introduction to Distributed Fiber Sensors* (CRC Press: Boca Raton, Florida (USA), 2017).

[4] R.W. Boyd, *Nonlinear Optics* (Academic Press, San Diego, CA - London, 2003).

[5] G. Agrawal, *Nonlinear Fiber Optics* (Academic Press, San Diego, CA, 2001).

[6] S. V. Shatalin, V.N. Treschikov, and A.J. Rogers, Appl. Opt. **37**, 5600 (1998).

[7] Y. Koyamada, M. Imahama, K. Kubota, and K. Hogari, J. Light. Technol. **27**, 1142 (2009).

[8] M.A. Soto and L. Thévenaz, Opt. Express **21**, 31347 (2013).

[9] M.A. Soto and F. Di Pasquale, in *Handb. Opt. Fibers* (Springer Nature, Singapore, 2018).

[10] G. Failleau, O. Beaumont, R. Razouk, S. Delepine-Lesoille, M. Landolt, B. Courthial, J.M. Hénault, F. Martinot, J. Bertrand, and B. Hay, Meas. J. Int. Meas. Confed. **116**, 18 (2018).

[11] Y. Muanenda, J. Sensors **2018**, 1 (2018).

[12] L. Palmieri and L. Schenato, Open Opt. J. **7**, 104 (2013).

[13] A. Motil, A. Bergman, and M. Tur, Opt. Laser Technol. **78**, 81 (2016).

[14] K.I. Aoyama, K. Nakagawa, and T. Itoh, IEEE J. Quantum Electron. **17**, 862 (1981).

[15] W. Eickhoff and R. Ulrich, Appl. Phys. Lett. **31**, 693 (1981).

[16] P. Jousset, T. Reinsch, T. Ryberg, H. Blanck, A. Clarke, R. Aghayev, G.P. Hersir, J. Henninges, M. Weber, and C.M. Krawczyk, Nat. Commun. **9**, 1 (2018).

[17] J.B. Ajo-Franklin, S. Dou, N.J. Lindsey, I. Monga, C. Tracy, M. Robertson, V.R. Tribaldos, C. Ulrich, B. Freifeld, T. Daley, and X. Li, Sci. Rep. **9**, 1 (2019).

[18] C. Yu, Z. Zhan, N.J. Lindsey, J.B. Ajo-Franklin, and M. Robertson, Geophys. Res. Lett. **46**, 1320

(2019).

[19] N.J. Lindsey, E.R. Martin, D.S. Dreger, B. Freifeld, S. Cole, S.R. James, B.L. Biondi, and J.B. Ajo-Franklin, Geophys. Res. Lett. **44**, 11,792 (2017).

[20] J. Ajo-Franklin, S. Dou, T. Daley, B. Freifeld, M. Robertson, C. Ulrich, T. Wood, I. Eckblaw, N.J. Lindsey, E.R. Martin, and A. Wagner, in *SEG Tech. Progr.* (2017), pp. 5223–5227.

[21] X. Zeng, C. Lancelle, C. Thurber, D. Fratta, H. Wang, N. Lord, A. Chalari, and A. Clarke, Bull. Seismol. Soc. Am. **107**, 603 (2017).

[22] S. Dou, N.J. Lindsey, A.M. Wagner, T.M. Daley, B. Freifeld, M. Robertson, J. Peterson, C. Ulrich, E.R. Martin, and J.B. Ajo-Franklin, Sci. Rep. **7**, 1 (2017).

[23] D. Arbel and A. Eyal, Opt. Express **22**, 8823 (2014).

[24] L. Shiloh and A. Eyal, Opt. Express **25**, 19205 (2017).

[25] N. Rawlinson, S. Pozgay, and S. Fishwick, Phys. Earth Planet. Inter. **178**, 101 (2010).

[26] Thorne Lay, editor , *Seismological Grand Challenges in Undestanding Earth's Dynamic Systems* (Report to the National Science Foundation. IRIS Consortium, 2009).

[27] J. Havskov, L. Ottemöller, A. Trnkoczy, and P. Bormann, in *New Man. Seismol. Obs. Pract.*, edited by P. Bormann (Deutsches GeoForschungsZentrum GFZ, Potsdam, Germany, 2012).

[28] F.C. Lin, D. Li, R.W. Clayton, and D. Hollis, Geophysics **78**, Q45 (2013).

[29] G. Marra, C. Clivati, R. Luckett, A. Tampellini, J. Kronjäger, L. Wright, A. Mura, F. Levi, S. Robinson, A. Xuereb, B. Baptie, and D. Calonico, Science (80-.). **361**, 486 (2018).

[30] Z. Pan, K. Liang, Q. Ye, H. Cai, R. Qu, and Z. Fang, Opt. Sensors Biophotonics **8311**, 83110S (2011).

[31] Z. Wang, L. Zhang, S. Wang, N. Xue, F. Peng, M. Fan, W. Sun, X. Qian, J. Rao, and Y. Rao, Opt. Express **24**, 853 (2016).

[32] J.C. Juarez and H.F. Taylor, Opt. Lett. **30**, 3284 (2005).

[33] A. Masoudi, M. Belal, and T.P. Newson, Meas. Sci. Technol. **24**, 1 (2013).

[34] J. Pastor-Graells, H.F. Martins, A. Garcia-Ruiz, S. Martin-Lopez, and M. Gonzalez-Herraez, Opt. Express **24**, 13121 (2016).

[35] M.R. Fernández-Ruiz, L. Costa, and H.F. Martins, Sensors **19**, 1 (2019).

[36] B. Lu, Z. Pan, Z. Wang, H. Zheng, Q. Ye, R. Qu, and H. Cai, Opt. Lett. **42**, 391 (2017).

[37] H.F. Martins, K. Shi, B.C. Thomsen, S. Martin-Lopez, M. Gonzalez-Herraez, and S.J. Savory, Opt. Express **24**, 22303 (2016).

[38] Z. Wang, B. Zhang, J. Xiong, Y. Fu, S. Lin, J. Jiang, Y. Chen, Y. Wu, Q. Meng, and Y. Rao, IEEE Internet Things J. **6**, 6117 (2018).

[39] C. Dorize and E. Awwad, Opt. Express **26**, 12878 (2018).

[40] H. Gabai and A. Eyal, Opt. Lett. **41**, 5648 (2016).

[41] A.E. Alekseev, V.S. Vdovenko, B.G. Gorshkov, V.T. Potapov, and D.E. Simikin, Laser Phys. **24**, (2014).

[42] Z. Sha, H. Feng, and Z. Zeng, Opt. Express **25**, 4831 (2017).

[43] G. Tu, X. Zhang, Y. Zhang, F. Zhu, L. Xia, and B. Nakarmi, IEEE Photonics Technol. Lett. **27**, 1349 (2015).

[44] D. Chen, Q. Liu, and Z. He, Opt. Express **25**, 8315 (2017).

[45] V. Torres-Company, D.E. Leaird, and A.M. Weiner, Opt. Express **19**, 24718 (2011).

[46] L. Costa, H.F. Martins, S. Martin-Lopez, M.R. Fernández-Ruiz, and M. Gonzalez-Herraez, J. Light. Technol. **37**, 4487 (2019).

[47] M.R. Fernández-Ruiz, H.F. Martins, L. Costa, S. Martin-Lopez, and M. Gonzalez-Herraez, J. Light. Technol. **36**, 5690 (2018).

[48] M.R. Fernández-Ruiz, J. Pastor-Graells, H.F. Martins, A. Garcia-Ruiz, S. Martin-Lopez, and M. Gonzalez-Herraez, J. Light. Technol. **36**, 979 (2018).

[49] A. Hartog, B. Frignet, D. Mackie, and M. Clark, Geophys. Prospect. **62**, 693 (2014).

[50] A. Mateeva, J. Lopez, H. Potters, J. Mestayer, B. Cox, D. Kiyashchenko, P. Wills, S. Grandi, K. Hornman, B. Kuvshinov, W. Berlang, Z. Yang, and R. Detomo, Geophys. Prospect. **62**, 679 (2014).

[51] D.C. Finfer, V. Mahue, S. V. Shatalin, T.R. Parker, and M. Farhadiroushan, in *SPE Annu. Tech. Conf. Exhib.* (Amsterdam, The Netherlands, 2014), pp. 1–5.

[52] T. Parker, S. Shatalin, and M. Farhadiroushan, First Break **32**, 61 (2014).

[53] T.M. Daley, B.M. Freifeld, J. Ajo-Franklin, S. Dou, R. Pevzner, V. Shulakova, S. Kashikar, D.E. Miller, J. Goetz, J. Henninges, and S. Lueth, Lead. Edge **32**, 699 (2013).

[54] C. Wang, in *SEG Tech. Progr.* (2018), pp. 5495–5499.

[55] B.N. Kuvshinov, Geophys. Prospect. **64**, 671 (2016).

[56] J.C. Hornman, Geophys. Prospect. **65**, 35 (2017).

[57] K.L. Feigl, C. Lancelle, D.D. Lim, L. Parker, E.C. Reinisch, S.T. Ali, D. Fratta, C.H. Thurber, H.F. Wang, M. Robertson, T. Coleman, D.E. Miller, J. Lopeman, P. Spielman, J. Akerley, C. Kreemer, C. Morency, and E. Matzel, in *43rd Work. Geotherm. Reserv. Eng.* (2018), pp. 1–15.

[58] E.R. Martin, F. Huot, Y. Ma, R. Cieplicki, S. Cole, M. Karrenbach, and B.L. Biondi, IEEE Signal Process. Mag. **35**, 31 (2018).

[59] F. Huot and B. Biondi, in *SEG Tech. Progr. Expand. Abstr. 2018* (2018), pp. 5501–5505.

[60] Z. Li and Z. Zhan, Geophys. J. Int. **215**, 1583 (2018).

[61] W. Zhu and G.C. Beroza, Geophys. J. Int. **216**, 261 (2018).

[62] Z.E. Ross, Y. Yue, M.A. Meier, E. Hauksson, and T.H. Heaton, J. Geophys. Res. Solid Earth **124**, 856 (2019).

[63] S.M. Hansen, B. Schmandt, A. Levander, E. Kiser, J.E. Vidale, G.A. Abers, and K.C. Creager, Nat. Commun. **7**, 1 (2016).

[64] Y. Ben-Zion, F.L. Vernon, Y. Ozakin, D. Zigone, Z.E. Ross, H. Meng, M. White, J. Reyes, D. Hollis, and M. Barklage, Geophys. J. Int. **202**, 370 (2015).

[65] L.M. Parker, C.H. Thurber, X. Zeng, P. Li, N.E. Lord, D. Fratta, H.F. Wang, M.C. Robertson, A.M. Thomas, M.S. Karplus, A. Nayak, and K.L. Feigl, Seismol. Res. Lett. **89**, 1629 (2018).

[66] E.F. Williams, M.R. Fernández-Ruiz, R. Magalhaes, Z. Zhan, M. Gonzalez-Herraez, and H.F. Martins, Nat. Commun. **in press**, (2019).

[67] H.F. Martins, M.R. Fernández-Ruiz, L. Costa, E. Williams, Z. Zhan, S. Martin-Lopez, and M. Gonzalez-Herraez, in *Opt. Fiber Commun.* (2019), pp. 1–3.

[68] M.R. Fernández-Ruiz, E.L. Williams, R. Magalhaes, R. Vanthillo, L. Costa, Z. Zhan, S. Martin-Lopez, M. Gonzalez-Herraez, and H.F. Martins, in *Proc. SPIE* (2019), pp. 1–4.

[69] J. Pastor-Graells, J. Nuno, M.R. Fernández-Ruiz, A. Garcia-Ruiz, H.F. Martins, S. Martin-Lopez, and M. Gonzalez-Herraez, J. Light. Technol. **35**, 4677 (2017).

[70] H.F. Martins, S. Martin-Lopez, P. Corredera, M.L. Filograno, O. Frazao, and M. Gonzalez-Herraez, J. Light. Technol. **31**, 3631 (2013).

[71] D. Information Technology, Https://Www.Cityofpasadena.Net/Wp-Content/Uploads/Sites/13/Fiber-Network-Map.Pdf (2017).

[72] E.R. Martin, N.J. Lindsey, J.B. Ajo-Franklin, and B. Biondi, EarthArXiv 1 (2018).

[73] H.F. Martins, S. Martin-Lopez, P. Corredera, J.D. Ania-Castañon, O. Frazao, and M. Gonzalez-Herraez, J. Light. Technol. **33**, 2628 (2015).

[74] M.R. Fernández-Ruiz, H.F. Martins, J. Pastor-Graells, S. Martin-Lopez, and M. Gonzalez-Herraez, Opt. Lett. **41**, 5756 (2016).

[75] F. Gyger, E. Rochat, and S. Chin, in *Opt. Fiber Sensors Conf.* (2014), pp. 91576Q 1–4.

[76] L. Zhang, L. Costa, Z. Yang, M.A. Soto, M. Gonzalez-Herraez, and L. Thévenaz, J. Light. Technol. 1 (2019).

[77] A. Sladen[1], D. Rivet[1], J.P. Ampuero[1], L. De Barros[1], Y. Hello[1], G. Calbris, and P. Lamare[3], EarthArXiv (2019).